

## MgO nanoparticles synthesized using chemical method for Skin cancer cell line(A375) cytotoxic assay

Nadia Jasim Ghdeeb<sup>1</sup>, Asma Hadi Mohammed<sup>2</sup>, Aseel Mustafa AbdulMajeed<sup>3</sup>

<sup>1,2</sup> Department of Physics, College of Science, Mustansiriyah University, Baghdad, Iraq([nadiajasim127@uomustansiriyah.edu.iq](mailto:nadiajasim127@uomustansiriyah.edu.iq), [asmaahadimohammed@yahoo.com](mailto:asmaahadimohammed@yahoo.com))

<sup>2</sup> Department of Physics, College of Science, Al-Nahrain University, Baghdad, Iraq, [aseelalaziz@uomustansiriyah.edu.iq](mailto:aseelalaziz@uomustansiriyah.edu.iq)

### ABSTRACT

Nano particles MgO with moral crystallinity were prepared by simple chemical method. Characterizations of the nano-products were done using X-ray diffraction (XRD) which confirmed the crystal-like nature of MgO NPs. More, field emission scanning electron microscope SEM has been used to demonstrate the morphology of the nanostructures of MgO NPs. The data yielded the average partical size of MgO NPs measured by SEM and XRD(30.145)nm and(6.529)nm respectively. Energy-dispersive X-ray spectroscopy (EDS) spectrum and XRD pattern confirmed that prepared MgO NPs were very pure. According to the MTT assay of A375 cells line the half maximal inhibitory concentration (IC<sub>50</sub>) is equal to 69.16 µg/mL .

**Key words:** magnesium oxide Nps, structure, morphological, skin cancer

*Article history:*

Received:    Received in revised format:    Accepted:    Available online:

### 1. Introduction

Nanotechnology is the pitch of science that studies produces at the nanoscale, generally among 1 and 100 nanometers. This technology brings diverse fields of science such as pharmaceuticals, dentistry, and bioengineering [1,2].

Nanoparticles have different properties compared to bulk materials. Most of the researchers work with metal oxide nanoparticles due to their unique properties such as hydrophobicity, photocatalyst, stability etc. Hence they are used in many applications named as coatings, catalysts, antibacterials, medical sciences, sensors, semiconductors, capacitors and batteries [3]. Metal oxides are of great concern to scientists, due to their improved surface composition and high surface area. Magnesium oxide (MgO) is one of the most important metal oxides with a wide range of applications in the refractory materials, coatings, superconducting industries, biological, electrochemical and medical fields.[4] Metal nanoparticles (NPs) have

<sup>\*</sup>Corresponding author : Nadia Jasim Ghdeeb<sup>1</sup>  
E-mail address: [nadiajasim127@uomustansiriyah.edu.iq](mailto:nadiajasim127@uomustansiriyah.edu.iq)

various applications in the biological, electrochemical, environmental, and medical fields [5,6].

Among oxide semiconductor nanoparticles, oxide of magnesium. Due to their chemical and physical properties, nanoparticles have gained significant importance in the field of gas sensors. MgO is a significant synthetic oxide that is considered safe for humans. MgO is a substance that is used in the medicine field for treatment of several diseases as an antacid and gastric acid [7,4].

The epidermis and dermis are the two main layers of skin. The epidermis is the skin's outermost layer, composed of melanocytes, keratinocytes, Merkel cells, and Langerhans cells [8]. Any irregularity in this layer will result in a variety of skin insults, including cancer. Skin cancer is classified into two broad categories: melanoma (cancers caused by melanocyte dysfunction) and non-melanoma skin cancers (from the epidermal derived cells) [9]. Melanoma develops as a result of abnormal cells of human melanocytes; pigment-containing cells that make up 90%, 5%, and 1% of the skin, eyes, and intestine, correspondingly. [10,11]. Melanoma accounts for less than 1% of all malignant skin cancers when compared to other skin insults. Despite recent advances in treatment, melanoma remains the most aggressive form of skin cancer, with a five-year existence rate of only 15–20 percent. [12,13]. Skin cancers other than melanoma (NMSC) caused by genetics and environment account for approximately 95% of all skin cancers. [14,15]. Nonmelanoma skin cancer encompasses a variety of other cancerous types, but these kinds are primarily classified into two subtypes: cutaneous squamous cell carcinoma (SCC) and basal cell carcinoma (BCC). Together, these two subtypes account for 99 percent of all NMSCs. [16]. Number of studies indicate that the global incidence of NMSC has increased by 3–8% per year since 1960 and is now 18–20 times greater than that of melanoma [17, 18]. Men are more likely than women to develop NMSC, and the risk of evolution is determined by genotypic, phenotypic, and environmental factors. [19] With the rising prevalence of skin cancer and the challenges associated with inefficient drug delivery systems, it is critical to expand the available methods for preventing or curing the disease.

The purpose of this research is to investigate the properties of metallic oxide (MgO Nps) and to ascertain its impact on skin cancer.

## **2. Materials and Methods**

Magnesium oxide nanoparticles were prepared by simple chemical method using magnesium nitrate and sodium hydroxide was obtained from (Central Drug House (P) Ltd.India).

the solution was prepared by adding (0.2 M) magnesium nitrate to (50 ml) deionized water. Then the solution was kept under constant stirring using magnetic stirrer for complete dissolution of contents. After complete dissolution, (0.2) M sodium hydroxide solution (50 ml) was added in drops along the sides of the container under constant stirring for 2 hours and the result is a milky precipitate, filtered and washed several times, left to dry and then burn the deposit in the oven at 400°C for 3 hours.

A number of examinations were carried out, including (XRD) was used SHIMADZU X-Ray diffractometer system (XRD-6000) which record the intensity as a function of Bragg's angle. The measurement settings are as follows Target: CuK $\alpha$ Wavelength = 1.5406 Å, Current=30 mA, Voltage=40 KV In the range of (20-80) with speed 10 (degree / min) with preset time = 0.30 (sec) , the scanning angle 2 $\theta$  shifted.

.Scanning electron microscopy was used to analyze agglomerations and other properties of the products, The samples have been examined by FESEM (EBSD Instrument: ZEISS SIGMA VP) in Daypetronic Co. Tehran-Iran. Atomic force microscopy is able to measure the nanometric scaling of insulating surfaces, as well as give 3D and 2D images of the surface and study the topography ,The model of AFM device is TT-2, Angstrom Advanced Inc, with a resolution of (0.3 nm) open loop piezo.Fourier transform infrared spectra are generated by the absorption of electromagnetic radiation in the frequency range (400 to 4000 cm<sup>-1</sup>). The frequency and intensity of absorption are the indications of the band structures and structural geometry of the molecule, as measured by Thermo Fisher Scientific Corporation's FT-IR at Daypetronic Co. in Tehran, Iran. Human Skin carcinoma (A375) cells were supplied by department of Pharmacology/ Faculty of Medicine, Centre for Natural Product Research and Drug Discovery, University of Malaya, A375 cell line is a human melanoma cell line initiated through explant culture of a solid tumor from a 54-year-old female. Store in liquid nitrogen (-196°C) until ready for experimental use. To check the cytotoxicity of MgO NPs on the A375 (1x10<sup>5</sup> ml<sup>-1</sup>) cells per well in their exponential growth phase, they were incubated for 24 hours with expanding MgO NPs concentrations, and the viability of the cells was quantified as a percentage of the untreated control (100 percent cell viability was investigated by MTT assay).

### 3.Result and Discussion

Figure (1) shows the XRD spectrum for the synthesized MgO nanoparticles .The presence of highly intense and multiple XRD peaks with broadening nature indicate that the product is well crystallized. On comparing with the standard diffraction pattern (Table 1), three distinguish peaks indexed to the cubic structure, JCPDS card No. 30-0794) for MgO nanoparticles [20,21]. These diffraction peaks at position 2 $\theta$  = 38.16 °, 44.8° and 58.8° belong to (222), (400) and (511) reflection planes respectively. The crystallite size (D) has been calculated for all peaks (Table 1) using Debye–Scherrer’s formula [22]:

$$D = 0.9\lambda / \beta \cos\theta \quad (1)$$

where  $\lambda$ ,  $\beta$  and  $\theta$  are the X-ray wavelength (1.5406 Å), full width at half maximum and Bragg diffraction angle respectively. The average crystallite size is found to be 6.529 nm.

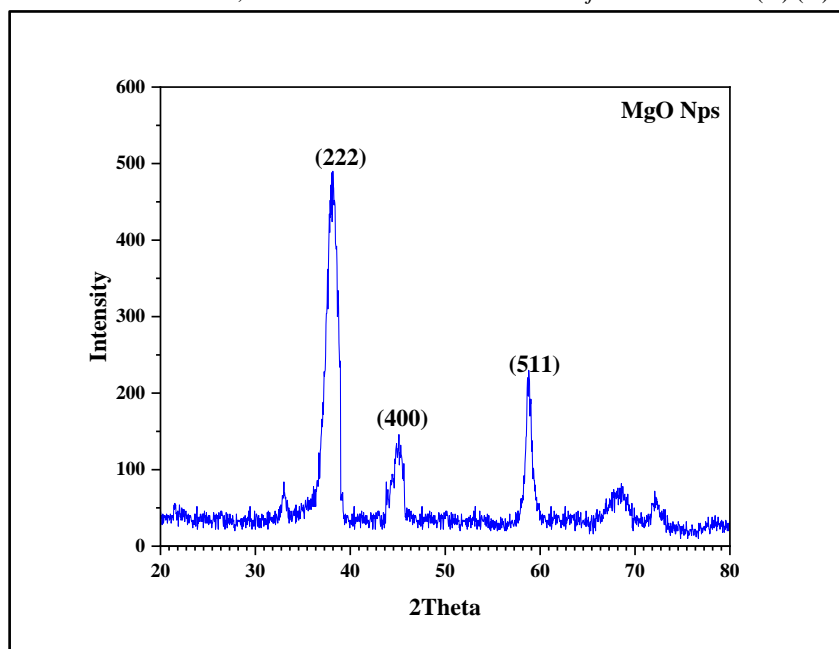


**Figure 1.** XRD pattern of MgO NPs

The title of the paper should be written in bold 14 point font, centered on the top of the paper. The first letter of every word in the title should be capitalized. The authors' names following the title, must be written in 12 point font (their affiliations in 10 point font).

Headings are capitalized. All major headings are flushed with the left margin in bold in 12 fonts. Do not put a period after the text of the heading. Leave one line above a major heading, and one line clear below before the start of the next paragraph or second-level heading. The whole paper should be written in “Times New Roman” font. The whole paper should be written in 12 point fonts. Every paragraph should be justified. Line spacing at paragraphs should be 1.15 cm, and please leave one line space between two paragraphs.

Please set the paper size as A4. Leave 2.54 cm margin at the top, 2.54 cm margin at the bottom of the page, 2.54 cm on both right and left sides. Please write your paper using Microsoft Office Word.

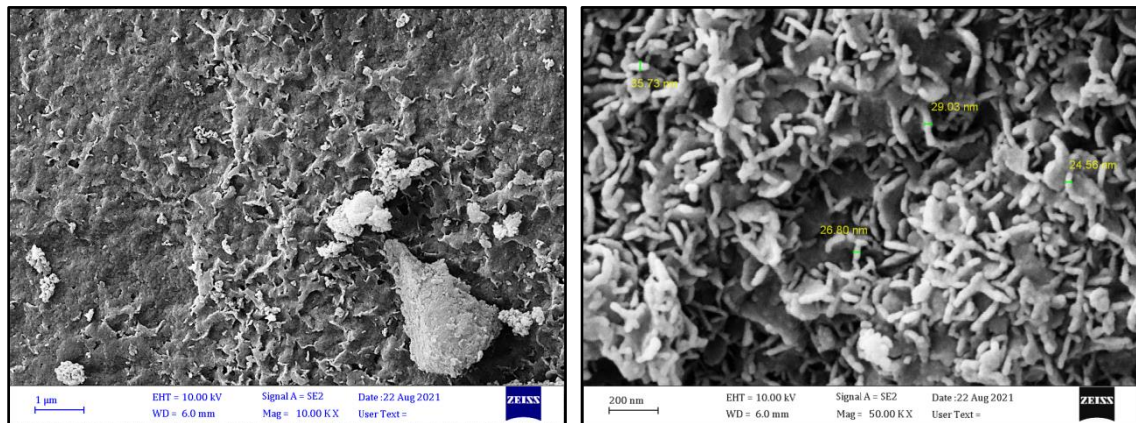
**Table 1.** The structural parameters of of MgO NPs.

<b>2θ stand (deg.)</b>	<b>2 θ Exp. (deg.)</b>	<b>FWHM (rad)</b>	<b>Miller indices (h k l)</b>	<b>D(nm)</b>
38.438	38.16	0.02452	0.385	(222)
44.369	44.8	0.01602	0.112	(400)
59.177	58.8	0.03745	0.188	(511)

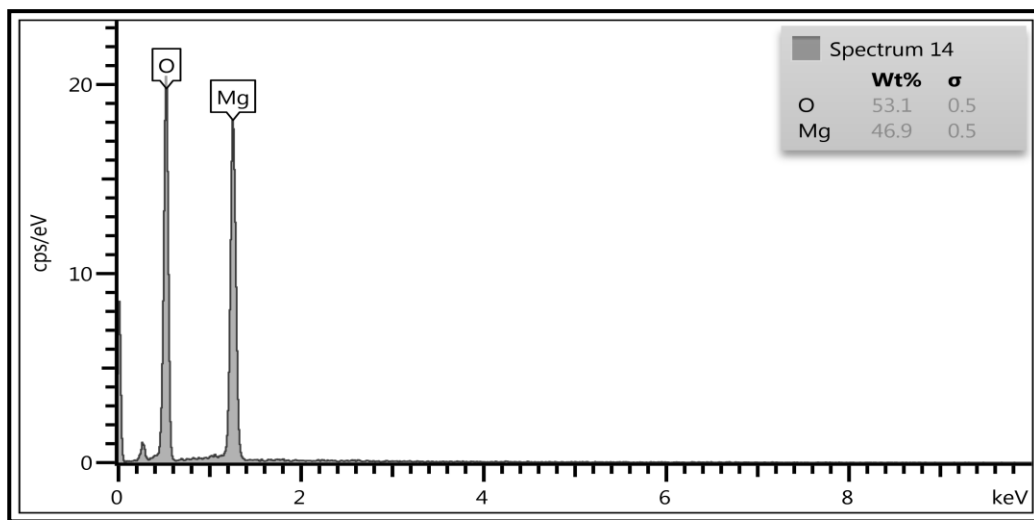
Figure (2) shows the surface morphology of the synthesized nanoparticles at two different

magnification scales (1  $\mu\text{m}$  and 200 nm). The grown particles are observed to be needle structure this result agrees with.[23]. The particle size of the MgO range between (24.56 - 35.73)nm.

The EDS spectrum Figure(3) of MgO nanoparticles indicates that the Mg and O elements are present in the sample.The weight ratio of Mg and O is found to be 46.9% and 53.1% which is inconsistent with the stoichiometry of MgO and slightly rich in oxygen content.



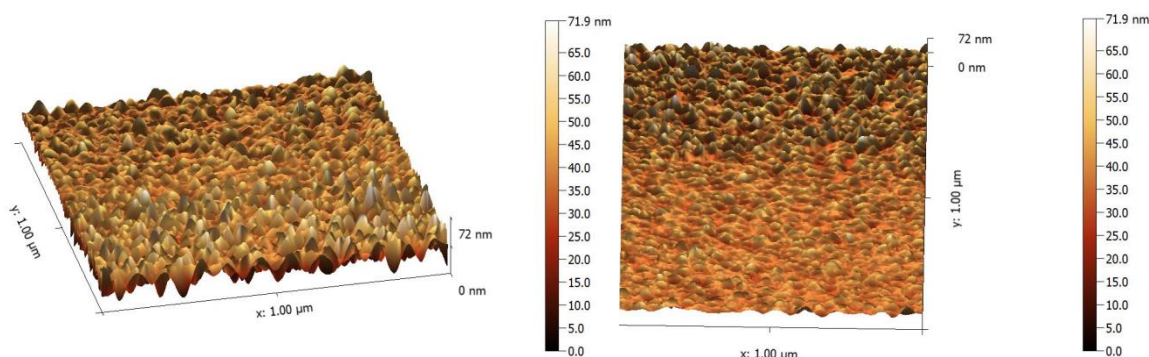
**Figure 2.** FE-SEM micrographs of MgO NPs at different magnification.



**Figure 3.** The EDX pattern of of MgO nanostructure

Figure (4) displays AFM images of Mg NPs, it is found that the roughness averages of MgO NPs 24.98 nm. The roughness is usually defined as closely spaced irregularities; it is measured by the vertical spacing of a real surface from its ideal form.

In the case where those spacing are large, then the surface can be defined as rough; otherwise, the surface can be defined as smooth. Average diameter are found by granularity cumulating distribution chart to be 67.54 nm.



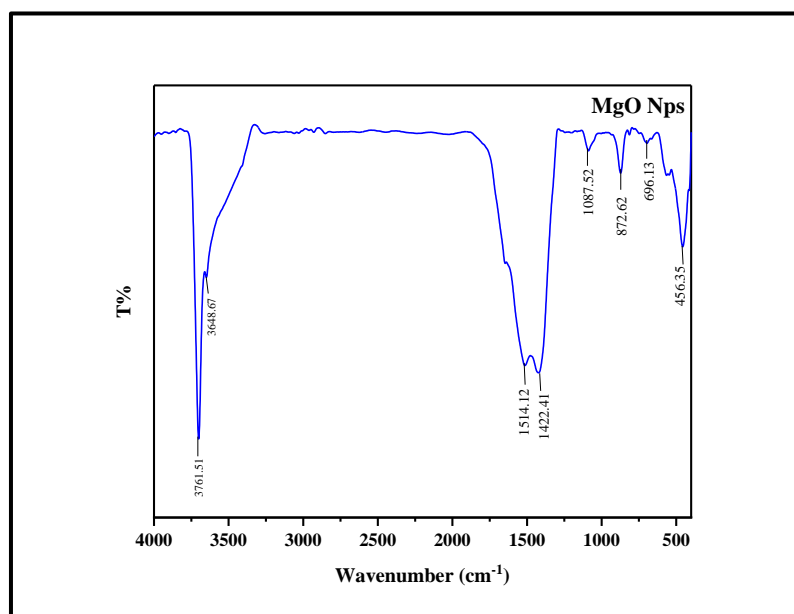
**Figure 4.** AFM images and histogram of MgO NPs

Figure (5) displays the FTIR spectrum of synthesized MgO NPs by chemical method. The observed bands identify the functional groups in MgO NPs, FTIR spectrum shows absorption intense bands at (3761.51,3648.67,1514.12,1422.41,1087.52, 872.62, 696.13, 456.35)  $\text{cm}^{-1}$ .

The strong infrared band near 3761.51-3648.67  $\text{cm}^{-1}$  is detected in the O - H bond vibrations of the hydroxy collection. The greatest intense band at 1514.12  $\text{cm}^{-1}$  denotes the C = O vibrations. The characteristic band is observed at wave number  $\sim 1422.41 \text{ cm}^{-1}$ , which is indicative of bending vibration

The surface hydroxyl group (Mg - OH). The range at 1087.52  $\text{cm}^{-1}$  corresponds to the C-N elongating of amines.

The broad band at  $456.35\text{ cm}^{-1}$  indicates the Mg-O vibration.[ 24,25]



**Figure 5.** Shows the FTIR of theMgO nanoparticle

Cytotoxicity results of A375cell viability after 72 hours of treatment with various concentrations of MgO NPs (6.25 to 400)  $\mu\text{g/mL}$  are shown in figure (6). All results indicated that, a decrease in cell viability in a dose-dependent manner, and MgO NPs solutions resulted in a significant decrease in the survival rate of A375cells in dose dependence ( $P < 0.0001$ ). The cytotoxicity results of MgO NPs are shown in Figure(6) and table (2). Cell viability loss was observed, which was dose-dependent. At a concentration of (6.25, 12.5)  $\mu\text{g/mL}$  for MgO NPs, there is no significant difference between A375carcinoma and normal cell WRL68. At higher concentrations (50 to 400  $\mu\text{g/mL}$ ) they observed a significant difference. The highest cell death rate of 32.82% was at the highest concentration of (400  $\mu\text{g/mL}$ ). The IC50 for MgO NPs was (69.16)  $\mu\text{g/mL}$  for A375and normal cell WRL68 was significantly higher (238.6)  $\mu\text{g/mL}$ .

**Table 2.** Viability (mean  $\pm$  standard deviation (SD) of syntheses MgONPs

Concen. ( $\mu\text{g/mL}$ )	A375		WRL68	
	Mean	$\pm\text{SD}$	Mean	$\pm\text{SD}$
400.00	32.82	2.77	71.95	0.81
200.00	42.43	5.12	84.80	1.20
100.00	53.39	5.77	93.60	2.10
50.00	62.22	3.34	95.33	1.18
25.00	79.78	4.65	95.22	0.82
12.50	96.76	1.14	95.95	1.03
6.25	96.30	0.81	95.95	0.20

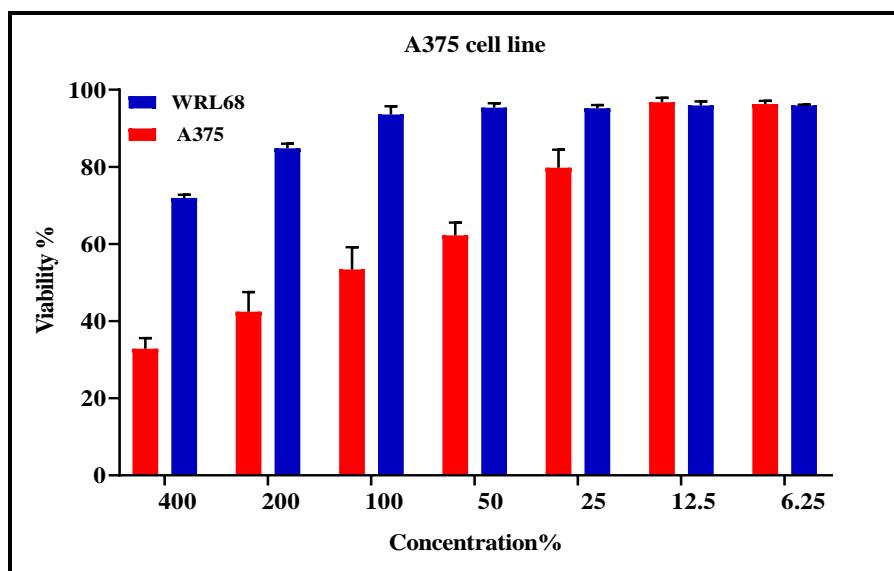


**Figure 6.** Cell Viability rate of synthesized MgO NPs A375 cell line

#### 4. Conclusion

The current study described simple method for the synthesis of MgONPs. The synthesized MgO NPs were subjected to different microscopic and spectroscopic investigations to ensure their nanostructures. The obtained results revealed the formation of nanoparticles with particle size of 30.145 nm and 6.529 nm . The synthesized cubical MgO nanoparticles showed good inhibition rate of A375 cancer cell lines.

#### References

- [1] Rafique M, Sadaf I, Rafique MS .(2017).green synthesis of silver nanoparticles and their applications. *Artif Cells Nanomed Biotechnol*, 45:1272–1291
- [2] Manne Anupama Ammulu, K. Vinay Viswanath, Ajay Kumar Giduturi, Praveen Kumar Vemuri. (2021) . Phytoassisted synthesis of magnesium oxide nanoparticles from *Pterocarpus marsupium* rox.b heartwood extract and its biomedical applications, *Journal of Genetic Engineering and Biotechnology* 19:21. [doi.org/10.1186/s43141-021-00119-0](https://doi.org/10.1186/s43141-021-00119-0)
- [3] K. Ganapathi Rao, CH. Ashok, K. Venkateswara Rao, CH. Shilpa Chakra. (2013) . Structural properties of MgO Nanoparticles: Synthesized by Co-Precipitation Technique, *International Journal of Science and Research (IJSR)*, 4.438, 43-46.
- [4] Hussain AA, Nazir S, Irshad R, Tahir K, Raza M, Khan ZUIH, Khan AU .( 2020). Synthesis of functionalized mesoporous Ni-SBA-16 decorated with MgO nanoparticles for Cr (VI) adsorption and an effective catalyst fo hydrodechlorination of chlorobenzene., *Mater Res Bull* ,(2020),133:111059. [doi.org/10.1016/j.materresbull.111059](https://doi.org/10.1016/j.materresbull.111059)
- [5] Kaur J, Singh J, Rawat M . (2019) .An efficient and blistering reduction of nitrophenol by green synthesized silver nanoparticles. *SN Appl Sci*, 1:1060. <https://doi.org/10.1007/s42452-019-1088-x>
- [6] Singh K, Kukkar D, Singh R, Kukkar P, Bajaj N, Singh J, Rawat M, Kumar A, Kim K-H. .(2020) . In situ green synthesis of Au/Ag nanostructures on a metalorganic framework surface for photocatalytic reduction of p-nitrophenol. *J Industr Eng Chem*,81:196–205. [doi.org/10.1016/j.jiec.2019.09.008](https://doi.org/10.1016/j.jiec.2019.09.008)
- [7] Kaur S, Singh J, Rawat R . (2018) .A smart LPG sensor based on chemobio synthesized MgO nanostructure. *J Mater Sci*,29:11679–11687.[doi. org/10.1007/s10854-018-9266](https://doi.org/10.1007/s10854-018-9266)

- [8] Losquadro WD. (2017).Anatomy of the skin and the pathogenesis of nonmelanoma skin cancer. *Facial Plastic Surgery Clinics* ,25(3):283–289.
- [9] Esteva A, Kuprel B, Novoa RA, Ko J, Swetter SM, Blau HM. (2017). Dermatologistlevel classification of skin cancer with deep neural networks. *nature*.542(7639):115-8.
- [10] Gray-Schopfer V, Wellbrock C, Marais R. ,(2007). Melanoma biology and new targeted therapy. *Nature* ,445(7130):851–7.
- [11] Pópulo H, Soares P, Lopes JM. (2012). Insights into melanoma: targeting the mTOR pathway for therapeutics. *Expert opinion on therapeutic targets*,16(7):689–705.
- [12] Siegel RL, Miller KD, Jemal A. . (2016). *Cancer statistics,CA: a cancer journal for clinicians*,66(1):7-30.
- [13] Society AC. *Cancer Facts & Figures*. 2017.
- [14] Didona D, Paolino G, Bottoni U, Cantisani C. (2018).Non melanoma skin cancer pathogenesis overview. *Biomedicine* 6(1):6.
- [15] Craythorne E, Al-Niami F. (2017). Skin cancer. *Medicine* ,45(7):431–4.
- [16] Green AC, Olsen C. (2017).Cutaneous squamous cell carcinoma: an epidemiological review. *Br J Dermatol* ,177(2):373–81.
- [17] Apalla Z, Lallas A, Sotiriou E, Lazaridou E, Ioannides D. (2017).Epidemiological trends in skin cancer. *Dermatology practical & conceptual*7(2):1.
- [18] Eide MJ, Krajenta R, Johnson D, Long JJ, Jacobsen G.(2010).Asgari MM,Identification of patients with nonmelanoma skin cancer using healthmaintenance organization claims data. *Am J Epidemiol* ,171(1):123–8.
- [19] Green A. (1992).Changing patterns in incidence of non-melanoma skin cancer. *Epithelial Cell Biol* ,1(1),47–51.
- [20] G. Balakrishnana, R. Velavana, Khalid Mujasam Batoob, Emad H. Raslancpp (2020). Microstructure, optical and photocatalytic properties of MgO nanoparticles, *Results in Physics* 16 ,103013 ,1-4.
- [21] Arass Jalal Noori, Fadil Abdullah Kareem.(2019) . The effect of magnesium oxide nanoparticles on the antibacterial and antibiofilm properties of glass-ionomer cement ,*Heliyon* 5,1-7.
- [22] C. B. Fitzgerald, M. Venkatesan, L. S. Dorneles, R. Gunning, P. ( 2006). Stamenov, and J.M. D. Coey, Magnetism in dilute magnetic oxide thin films based on SnO<sub>2</sub>," *PHYSICAL REVIEW* ",B 74,115307 .
- [23] Sharma, G., R. Soni, and N.D. Jasuja.(2017).Phytoassisted synthesis of magnesium oxidenanoparticles with *Swertia chirayaita*. *Journal of Taibah University for Science* , 11(3): 471-477.
- [24] G. Balakrishnana , R. Velavana, Khalid Mujasam Batoob, Emad H. Raslanc . (2020). Microstructure, optical and photocatalytic properties of MgO nanoparticles , *Results in Physics* 16 ,103013 ,1-4.
- [25] Renata Dobrucka . (2018) . Synthesis of MgO Nanoparticles Using *Artemisia abrotanum* Herba Extract and Their Antioxidant and Photo catalytic Properties, *Iran J Sci Technol Trans Sci*. 42,547–555